

Tunneling Dendrimers. Enhancing Charge Transport through Insulating Layer Using Redox Molecular Objects

Sébastien Lhenry,[†] Joanna Jalkh,[†] Yann R. Leroux,[†] Jaime Ruiz,[‡] Roberto Ciganda,[‡] Didier Astruc,[‡] and Philippe Hapiot^{†,*}

[†]Institut des Sciences Chimiques de Rennes, CNRS, Université de Rennes 1, UMR 6226 (Equipe MaCSE), Campus de Beaulieu, 35042 Rennes Cedex, France

[‡]Institut des Sciences Moléculaires, Université Bordeaux 1, CNRS, UMR 5255, 33405 Talence Cedex, France

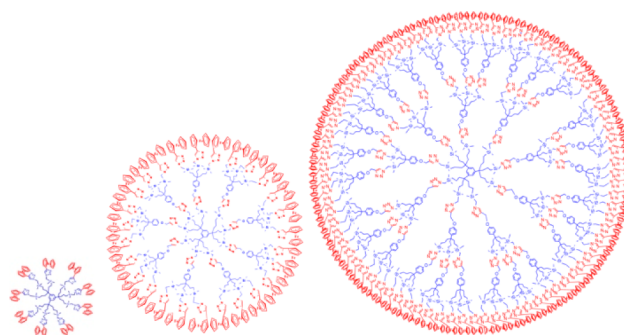
S Supporting Information

ABSTRACT: Charge transport through an insulating layer was probed using ferrocenyl-terminated dendrimers and scanning electrochemical microscopy. Experiments show that the passage through the layer is considerably enhanced when the transferred charges are brought globally to the surface by the ferrocenyl dendrimer instead of a single ferrocene molecule. This result shows that charge tunneling through an insulator could be promoted by a purely molecular nano-object.

Several recent studies have highlighted that the charge transfer through an insulating layer from a molecule present in solution to a substrate could be restored by attaching a few nanoparticles^{1–4} and even a single nanoparticle on the outside of an insulating layer.^{5,6} Theoretical analyses have provided some explanations to understand the origins of this phenomenon.^{7,8} A higher density of state in a metallic nanoparticle enhances the electron tunneling across the insulating layer and thus the global kinetics of electron transfer. In other words, tunneling from a nanoparticle to a substrate is much more probable than tunneling from single molecules. Beside the fundamental consequences of this observation, it has already opened a route to the developments of novel analytical methods, whereby a nanoparticle deposited on an insulating layer behaves as a functional nanoelectrode.^{5,6}

Looking back in literature, the phenomenon has been observed several times for other nanostructures like nanotube⁹ or graphene oxide¹⁰ that could behave as an electronic nanocollector in such a configuration. In this context, we could wonder if purely molecular objects containing a large number of redox centers are similarly able to enhance the charge transfers through an insulating barrier. This is a fundamental problem, as it means that the insulating protection of a layer or of a membrane clearly depends on how charges are brought to the surface of the barrier. In this work, we have considered the example of redox dendrimers terminated by ferrocenyl centers (Scheme 1). Redox dendrimers represent a large class of molecular objects with numerous possibilities to obtain a desired function by the adaptation of their topology and the possibility of introducing specific redox-active metal centers.^{11–16} Interestingly for the present use, efficient and fast electrochemical communication occurs between the redox centers immobilized on the outside edge of the dendrimer, making that such multiple-redox systems

Scheme 1. Structures of the Redox Dendrimer Molecules As G0 (9-Ferrocenyl), G1 (27-Ferrocenyl), and G2 (81-Ferrocenyl)



generally appear as a single multielectronic redox system (for example, they display a single peak in cyclic voltammetry).^{17,18}

We used scanning electrochemical microscopy (SECM) in feedback mode for probing charge transfers through an insulating layer.^{19,20} In this technique, the active form of the mediator is formed at the tip electrode that is maintained at the vicinity of the sample. The mediator diffuses to the sample where it could exchange its charge with the substrate through the insulating layer. If charge transfer occurs at the surface of the sample, the concentration profile of the mediator is modified resulting in a change of the current at the tip electrode that increases with the tip–substrate distance d . Thus, by varying the nature of the mediator, we could evaluate the charge transfer efficiency through the insulating layer in mono- and multielectronic systems.

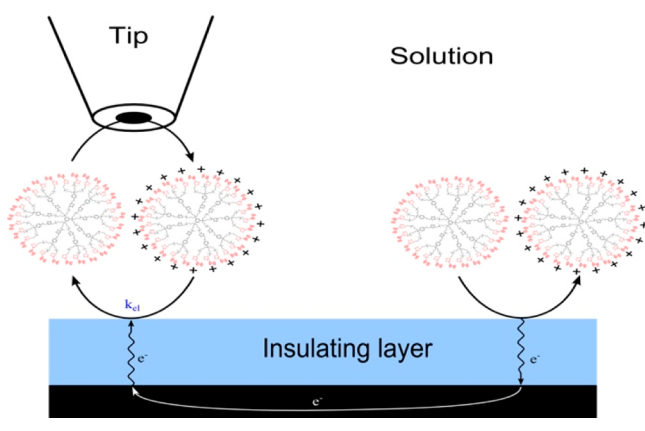
Our SECM experiments were performed in unbiased conditions, meaning that the substrate is not electrically connected. In steady state SECM to balance the charges injected in the sample, charges must return to the solution after transport through the substrate to outside the diffusion cone of the tip electrode. We could thus expect a good sensitivity of the method versus changes of the tunneling because the charges must pass several times though the insulating layer (see Scheme 2).

As mediators, we considered three different generations of ferrocenyl-terminated dendrimers (noted as G0, G1, and G2

Received: October 27, 2014

Published: December 12, 2014

Scheme 2. Evaluation of the Charge Transfer Kinetics Using SECM in Unbiased Feedback Mode



with 9, 27, and 81 ferrocene (Fc) sites per molecule, respectively) and ferrocene itself. In most of the previously published studies, the insulating layer was a self-assembled monolayer as the preparation of a blocked metallic electrode with long thio-alkyl chain is an easy-to-handle process.^{1,5} However, the presence of defects as well as the dynamic nature of such a layer that permits reorganization when large objects are immobilized on the layer may create difficulties in detailed analysis or for practical applications in electrode construction.^{21,22} For this reason, we used a different type of layer prepared by electrografting of an aryl diazonium salt (4-(ethynyl)benzenediazonium salt) on a flat carbon substrate.²³ As discussed before, when molecules are covalently attached onto a carbon surface, they stay in a sort of frozen arrangement.²⁴ After modification, the sample appears as a flat, homogeneous surface with a low roughness.²⁴

Ferrocene is a classical SECM mediator, but using multiredox molecules as mediator is less common. Thus, a first experiment has concerned the response of a redox dendrimer when used as a SECM mediator. Figure 1 shows some SECM approach curves (variation of the normalized current i/i_{inf} with the normalized distance $L = d/a$ where i_{inf} is the current at the tip when the tip is far from the sample, and a is the tip radius = 5 μm) recorded using the G0, G1, and G2 dendrimers and ferrocene (Fc) on an insulating surface (glass) and on an unmodified conducting pyrolyzed photoresist film (PPF).²⁵ For Fc, G0, and G1, experimental data fit well the behaviors expected for a totally insulating and conducting substrate. A slight discrepancy is visible for curves recording with G2 that may indicate some adsorption of G2 on the glass substrate and 2D-transport between adsorbed dendrimers (see below).²⁶

In a second stage, polyphenylene layers are deposited on PPF substrates. Changing the conditions of the grafting (time and applied potentials) permits the variation of the deposited layer thickness.²³ The quality of the layer, especially about the possible presence of defects, was checked using a common test in which a cyclic voltammogram of the oxidation of ferrocene is recorded, the modified surface serving as an electrode (see Figure S3 in the Supporting Information). The modified surfaces are then examined by SECM using the full series of mediators. Figure 2 shows curves recorded for a surface covered with a thick layer (top) and a thin layer (bottom). Thicknesses of the two layers were estimated by AFM scratching²⁷ following published procedures around 5 nm and around 2 nm for the thick and the thin layers, respectively. Approach curves recorded on the PPF substrate with the thick layer show a negative feedback with

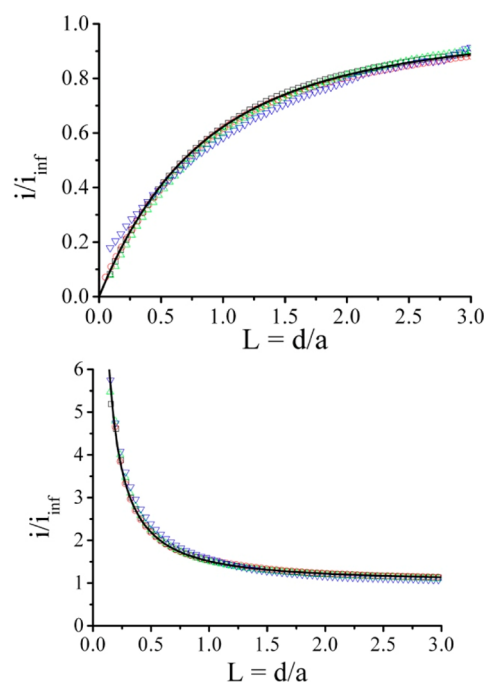


Figure 1. SECM approach curves recorded on glass (top) and PPF substrates (bottom) recorded in $\text{CH}_2\text{Cl}_2 + 0.2 \text{ mol L}^{-1} n\text{-Bu}_4\text{NPF}_6$ with ferrocene ($10^{-3} \text{ mol L}^{-1}$) (black \square); G0 ($1.1 \times 10^{-4} \text{ mol L}^{-1}$) (red \circ); G1 ($3.7 \times 10^{-5} \text{ mol L}^{-1}$) (green \triangle); and G2 ($1.23 \times 10^{-5} \text{ mol L}^{-1}$) (blue ∇). Lines are the theoretical behavior predicted for an insulating (negative feedback, top) and conducting substrates (positive feedback, bottom).

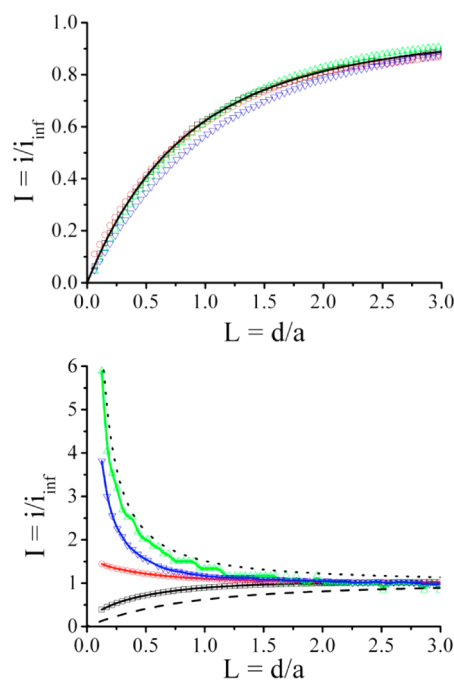


Figure 2. Approach curves recorded on PPF substrates modified with a thick (top) and thin (bottom) organic layers in $\text{CH}_2\text{Cl}_2 + 0.2 \text{ mol L}^{-1} \text{Bu}_4\text{NPF}_6$ with ferrocene ($10^{-3} \text{ mol L}^{-1}$) (black \square); G0 ($1.1 \times 10^{-4} \text{ mol L}^{-1}$) (red \circ); G1 ($3.7 \times 10^{-5} \text{ mol L}^{-1}$) (green \triangle); and G2 ($1.23 \times 10^{-5} \text{ mol L}^{-1}$) (blue ∇). Dashed lines are the theoretical behaviors for an insulating (negative feedback) and conducting substrate (positive feedback).

all the mediators (the current decreases with the tip–substrate distance) indicating the absence of regeneration of the mediator on the sample as observed for the insulating glass sample of Figure 1. This shows that the electrode surface is totally blocked by the thick insulating layer, which is expected considering its estimated thickness. On the thin layer substrate, the curve recorded with the ferrocene mediator corresponds to a very slow charge transfer (the corresponding dimensionless rate constant κ could be estimated as 0.05), which agrees with previous data, as the layer is not sufficiently thick for totally annihilating the possibility of charge tunneling.²⁴ However, it also shows the quasi-absence of pinholes/defects in our layer or the occurrence of an efficient 2D-transport that both would result in a positive feedback as observed before for a specially designed carboxylated layer where the density of redox dendrimers is high.²⁶

A different behavior is detected when the surface is examined with the three dendrimer mediators (see Figure 2 bottom). Large increases of the positive feedback characters are now visible in the order $G1 > G2 > G0 > Fc$. Notice that the equivalent concentration of ferrocene groups was kept the same for all the experiments (10^{-3} mol L⁻¹). Such variations demonstrate that the charge transfer rate through the insulating layer is greatly enhanced when the charges are brought to the surface by the ferrocenyl dendrimers by comparison with a single ferrocene molecule. As seen in Figure 2 (bottom) for the G1 dendrimer, the charge transfer at the modified surface is so efficient that it is close to that expected on PPF in the absence of an insulating organic layer. As it was proposed for metallic nanoparticles, we could connect this effect to an increase of the density of redox centers due to the simultaneous access of several equivalent redox entities. We could reject that the restoration of the charge transfer at the surface originates from the permeation of the dendrimer through pinholes or defects. Indeed, it is excluded that dendrimers that are 10 nm size objects could pass through pinholes of an organic layer better than a single ferrocene molecule.

We observe an increase of the effect with the dendrimer generation, meaning with the number of ferrocene moieties ($G1 > G0 > Fc$). If redox dendrimers are nano-objects, they are different from metallic nanoparticles. As it was shown in a case of Ru-based redox dendrimers when increasing their size, not all redox centers are immediately available because of limitations of the charge transport kinetics along their spheric core.¹⁸ A similar phenomenon is probably at the origin of the slight charge transfer decrease observed from G1 to G2 meaning that an optimization of the dendrimer structure is required.

In summary, these are preliminary experiments showing that purely molecular objects are indeed able to enhance the charge-tunneling transport through an insulating layer. They prove the general character of the phenomena that is not reserved to metallic nanoparticles, nanotubes, or graphene nanosheets. Kinetics enhancements also exist with a nano-object containing multiple discrete charge carriers suggesting some adaptations of the theoretical view of the phenomena. Nevertheless, for practical applications, considering the possibilities in the design of such molecular nano-objects, it opens a route to novel developments combining nanoscience (like those recently proposed for single metallic nanoparticles on a nanoelectrode)⁵ and chemical reactivity. Additional experiments are obviously required to understand the roles of the dendrimer topology, the nature of different redox centers, and a better identification of the parameters that control or limit the phenomena.

■ ASSOCIATED CONTENT

📄 Supporting Information

Experimental details about the SECM procedure, chemicals, preparation, and cleaning of the modified surface are described. This material is available free of charge via the Internet at <http://pubs.acs.org>.

■ AUTHOR INFORMATION

Corresponding Author

*philippe.hapiot@univ-rennes1.fr

Notes

The authors declare no competing financial interest.

■ ACKNOWLEDGMENTS

Dr. Jean-François Bergamini is warmly thanked for his help in the thickness measurement by AFM-scratching and AFM surface characterizations.

■ REFERENCES

- (1) Dyne, J.; Lin, Y. S.; Lai, L. M. H.; Ginges, J. Z.; Luais, E.; Peterson, J. R.; Goon, I. Y.; Amal, R.; Gooding, J. J. *ChemPhysChem* **2010**, *11*, 2807–2813.
- (2) Kissling, G. P.; Miles, D. O.; Fermin, D. J. *Phys. Chem. Chem. Phys.* **2011**, *13*, 21175–21185.
- (3) Kissling, G. P.; Bunzli, C.; Fermin, D. J. *J. Am. Chem. Soc.* **2010**, *132*, 16855–16861.
- (4) Gambardella, A. A.; Feldberg, S. W.; Murray, R. W. *J. Am. Chem. Soc.* **2012**, *134*, 5774–5777.
- (5) Kim, J.; Kim, B.-K.; Cho, S. K.; Bard, A. J. *J. Am. Chem. Soc.* **2014**, *136*, 8173–8176.
- (6) Yu, Y.; Gao, Y.; Hu, K.; Blanchard, P.-Y.; Noël, J.-M.; Nareshkumar, T.; Phani, K. L.; Friedman, G.; Gogotsi, Y.; Mirkin, M. V. *ChemElectroChem* **2014**, DOI: 10.1002/celc.201402312.
- (7) Chazalviel, J.; Allongue, P. *J. Am. Chem. Soc.* **2010**, *133*, 762–764.
- (8) Barfidokht, A.; Ciampi, S.; Luais, E.; Darwish, N.; Gooding, J. J. *Anal. Chem.* **2013**, *85*, 1073–1080.
- (9) Hauquier, F.; Pastorin, G.; Hapiot, P.; Prato, M.; Bianco, M.; Fabre, B. *Chem. Commun.* **2006**, 4536–4538.
- (10) Zhang, B.; Fan, L.; Zhong, H.; Liu, Y.; Chen, S. *J. Am. Chem. Soc.* **2013**, *135*, 10073–10080.
- (11) Astruc, D. *Nat. Chem.* **2012**, *4*, 255–267.
- (12) Ornelas, C.; Ruiz, J.; Belin, C.; Astruc, D. *J. Am. Chem. Soc.* **2009**, *131*, 590–601 and references therein.
- (13) Takada, K.; Díaz, D. J.; Abruña, H. D.; Cuadrado, I.; Casado, C.; Alonso, B.; Morán, M.; Losada, J. *J. Am. Chem. Soc.* **1997**, *119*, 10763–10773.
- (14) Amatore, C.; Grun, F.; Maisonhaute, E. *Angew. Chem., Int. Ed.* **2003**, *42*, 4944–4947.
- (15) Kaifer, A. E. *J. Inorg. Chem.* **2007**, *32*, 5015–5027 and references therein.
- (16) Ornelas, C.; Ruiz, J.; Cloutet, E.; Alves, S.; Astruc, D. *Angew. Chem., Int. Ed.* **2007**, *46*, 872–877.
- (17) Oh, S.-K.; Baker, L. A.; Crooks, R. M. *Langmuir* **2002**, *18*, 6981–6987.
- (18) Amatore, C.; Bouret, Y.; Maisonhaute, E.; Goldsmith, J. I.; Abruña, H. D. *Chem.—Eur. J.* **2001**, *7*, 2206–2226.
- (19) Bard, A. J.; Mirkin, M. V. *Scanning Electrochemical Microscopy*; Marcel Dekker: New York, 2001.
- (20) Wittstock, G.; Burchardt, M.; Sascha, E. P.; Shen, Y.; Zhao, C. *Angew. Chem., Int. Ed.* **2007**, *46*, 1584–1617.
- (21) Wackerbarth, H.; Grubb, M.; Zhang, J.; Hansen, A. G.; Ulstrup, J. *Langmuir* **2004**, *20*, 1647–1655.
- (22) Liu, B.; Bard, A. J.; Mirkin, M. V.; Creager, S. E. *J. Am. Chem. Soc.* **2004**, *126*, 1485–1492.
- (23) Pinson, J.; Bélanger, D. *Chem. Soc. Rev.* **2011**, *40*, 3995–4048.

- (24) Leroux, Y. R.; Fei, H.; Noël, J.-M.; Roux, C.; Hapiot, P. *J. Am. Chem. Soc.* **2010**, *132*, 14039–14041.
- (25) McCreery, R. L. *Chem. Rev.* **2008**, *108*, 2646.
- (26) Wang, A. F.; Ornelas, C.; Astruc, D.; Hapiot, P. *J. Am. Chem. Soc.* **2009**, *131*, 6652–6653.
- (27) Anariba, F.; DuVall, S. H.; McCreery, R. L. *Anal. Chem.* **2003**, *75*, 3837–3844.